Chemical Engineering Science 295 (2024) 120142

Contents lists available at ScienceDirect

Chemical Engineering Science

journal homepage: www.elsevier.com/locate/ces

Mass transport in Couette flow

A.S. Hamilton-Morris, S.C. Generalis, P.T. Griffiths, P.M.J. Trevelyan *

Applied Mathematics and Data Science, Aston University, B4 7ET, UK

ARTICLE INFO

Keywords:
Mass transport
Diffusion
Couette flow
Effective diffusivity

ABSTRACT

In this study we examine the large Péclet number, Pe, limit of a concentration boundary layer in Couette flow. The boundary layer has a thickness of order $Pe^{-1/2}$. The asymptotic concentration is asymptotically obtained as an integral solution up to order $Pe^{-1/2}$ using the Fourier sine transform. The asymptotic solution is found to be in good agreement with the full numerical solution for large Péclet numbers. Further, the effective diffusivity obtained from the asymptotic solution is found to be in good agreement with the effective diffusivity obtained from the full numerical solution for large Péclet numbers.

1. Introduction

Heat and mass transport play an important role in many fields including geophysical flows (Helffrich and Wood, 2001), oceanography (Zhang et al., 2014), and atmospheric sciences (Pithan et al., 2018). Many industries involve mass transport, for example the food industry, which aim to efficiently mix the ingredients to produce a uniform/homogeneous mixture (Wang and Sun, 2003), the paint industry use mixing to create emulsions which are a stable mixture of an aqueous fluid with an oil (Zhao et al., 2022), and the energy sector for fuel cells (Siegel, 2008). The pharmaceutical industry uses animal cells to produce antibodies or yeast, such fragile and delicate products need to be treated more carefully when mixing is required, for example to ensure the active samples have an oxygen supply (Butler, 2005).

There are numerous of studies on heat/mass transport enhancement in the presence of chaotic flows, as they provide efficient mixing and so are widely used in industry. Ghosh et al. (1992) examined heat transfer enhancement between two rotating eccentric cylinders held at different temperatures. The resulting flow was chaotic and they found an expression for the effective diffusivity as an expansion in the eccentricity in the large Péclet number, Pe, limit. The Péclet number is the product of the length scale and velocity scale divided by the diffusion coefficient. Bryden and Brenner (1999) numerically examined the chaotic motion inside a spherical droplet using Stokes flow in the presence of an external shear force. Grassia and Ubal (2018) numerically examined the mass transport across a spherical droplet in the large Péclet number limit. They introduced a streamline averaging technique in which concentrations varied between streamlines but not on streamlines.

Pöschke et al. (2017) examined the two dimensional flow in a periodic cat eyes pattern in the large Péclet number limit where the boundary layer scaled with $Pe^{-1/2}$. This study numerically examined the mean square displacement and found that several different time scales were present.

In this study we examine mass transport in Couette flow. This is laminar flow in the gap between two concentric cylinders where the outer cylinder is rotating and the inner cylinder is stationary. One notes that when both cylinders rotate, the flow is called Taylor-Couette flow which has been the centre of attention in a plethora of studies due to the various possible flow regimes, for example see Taylor (1923); Coles (1965); Andereck et al. (1986); Hristova et al. (2002); Nemri et al. (2016); Godwin et al. (2023) for more details on this. An analytical expression for the stability of Taylor-Couette flow was given by Esser and Grossmann (1996).

Many different flows have been investigated to examine mass transport especially in the large Péclet number limit. Acrivos and Goddard (1965) studied flow over a semi-infinite plate and found that the concentration boundary layer thickness scaled with $Pe^{-1/3}$. This result was used by Trevelyan et al. (2002) in a square cavity with a concentration difference on the stationary walls but with internally generated flow, to obtain the effective diffusivity in the large Pe limit as $D_{\text{eff}} = 1.1613 D \text{Pe}^{1/3}$ where D is the molecular diffusion coefficient. Additionally, Trevelyan et al. (2002) found that in Couette flow with a concentration difference on the stationary outer cylinder, with the inner cylinder moving, that the effective diffusivity in the large Pe limit was $D_{\text{eff}} = 0.6741 D(\phi \text{Pe})^{1/3}$ where $\phi = \kappa/[\pi(1-\kappa)^2(1+\kappa)]$ and $\kappa = a/b$ where the inner and outer cylinder radii are a and b, respectively.

* Corresponding author.
E-mail address: p.trevelyan@aston.ac.uk (P.M.J. Trevelyan).

https://doi.org/10.1016/j.ces.2024.120142
Received 23 December 2023; Received in revised form 26 March 2024; Accepted 17 April 2024
Available online 25 April 2024

When the concentration difference is on a moving boundary, then the concentration boundary layer thickness scales with $\mathrm{Pe}^{-1/2}$. A very intuitive study was performed by Shraiman (1987) on mass transport across Rayleigh-Bénard cells and they found that in the large Péclet number limit, that the effective diffusivity was given by $D_{\text{eff}} = 0.487D\sqrt{\mathrm{Pe}\pi w/k}$ where k is the wavelength of the cell. This result was a more accurate version of the result obtained by Rosenbluth et al. (1987). One notes that for perfect chaotic mixing the effective diffusivity scales with the Péclet number (Thiffeault, 2012). Further, for shear flows, Taylor (1953); Aris (1956) found that the effective diffusivity scaled with the Péclet number squared.

In this study we examine the effective diffusivity in Couette flow. In section 2 the model equations are presented and non-dimensionalised. In section 3 the system of equations is expanded in the large Péclet number limit. In section 4 the zeroth order solution is obtained using a superposition of a similarity solution and an integral solution obtained using the Fourier sine transform. In section 5, the first order correction to the zeroth order solution is obtained. In section 6, the effective diffusivity is obtained using the zeroth and first order solutions. In section 7, the full problem is numerically solved. The effective diffusivity for the numerical solution is compared with the large Pe number asymptotic limit. In section 8, we draw our conclusions. In appendix A, the Fourier sine transform is given. In Appendix B, we apply the same analysis to planar Couette flow with a periodic concentration specified on a moving wall.

2. Model

Suppose we have two concentric cylinders centred at the origin. The inner cylinder of radius a is stationary, whilst the outer cylinder of radius b is rotating anti-clockwise with an angular velocity of w_0. We suppose a fluid is between the two cylinders with constant density ρ and kinematic viscosity ν. We assume that the fluid satisfies the incompressible Navier-Stokes equations. A species C with molecular diffusion coefficient D will dissolve into the fluid. We assume that the concentration is sufficiently dilute that saturation effects can be neglected so that the concentration c satisfies the mass transport equation. We assume that the species does not affect the density or viscosity of the fluid, hence we have the bulk equations:

$$\underline{\nabla}\cdot\underline{u} = 0, \tag{1}$$

$$\underline{u}_t + (\underline{u}\cdot\underline{\nabla})\underline{u} = -\frac{1}{\rho}\underline{\nabla}p + \nu\nabla^2\underline{u}, \tag{2}$$

$$c_t + (\underline{u}\cdot\underline{\nabla})c = D\nabla^2 c \tag{3}$$

where subscripts denote partial derivatives, $\underline{u}$ is the fluid velocity, p is the fluid pressure and t is time. We suppose the inner stationary cylinder is impermeable so that we have the no slip and no flux boundary conditions:

$$c_r = 0 \quad \text{and} \quad \underline{u} = \underline{0} \quad \text{on} \quad r = a \tag{4}$$

where r is the radial coordinate measured from the origin. For clarity, the x-axis is horizontal and the y-axis is vertical. The outer cylinder is assumed permeable. We suppose that there is a large container, surrounding the upper half of the outer cylinder, containing species C at the concentration c_0. Thus, on the upper half of the outer cylinder, $y > 0$, we shall assume that species C is held at a constant concentration c_0. We suppose that there is a large amount of catalyst held in the region below the outer cylinder such that when species C makes contact with the catalyst it undergoes a fast first order chemical reaction. We suppose that the reaction rate of the chemical reaction is sufficiently fast that it can be assumed instantaneous. Thus, on the lower half of the outer cylinder, $y < 0$, we shall assume that species C is absent. Hence, on the outer cylinder we have the boundary conditions:

$$c = \begin{cases} c_0 & \text{for} \quad 0 \le \theta < \pi \\ 0 & \text{for} \quad \pi \le \theta < 2\pi \end{cases} \quad \text{and} \quad \underline{u} = w_0\underline{e}_\theta \quad \text{on} \quad r = b \tag{5}$$

where θ is the angle measured from the positive x-axis in the anti-clockwise direction.

As this problem involves circular boundaries we shall express the equations in cylindrical polar coordinates. We assume that the flow and concentration have reached a steady state, i.e. $c_t = 0$ and $\underline{u}_t = \underline{0}$. Further, we assume that the flow field is purely rotational and so takes the form $\underline{u} = w(r)\underline{e}_\theta$, where $\underline{e}_\theta$ is the unit vector in the θ direction. Then the incompressibility condition is already satisfied and the bulk equations become

$$-\frac{w^2}{r} = -\frac{1}{\rho}\frac{\partial p}{\partial r}, \tag{6}$$

$$0 = -\frac{1}{\rho r}\frac{\partial p}{\partial \theta} + \nu\left[\frac{1}{r}\frac{d}{dr}\left(r\frac{dw}{dr}\right) - \frac{w}{r^2}\right], \tag{7}$$

$$\frac{w}{r}\frac{\partial c}{\partial \theta} = D\left[\frac{1}{r}\frac{\partial}{\partial r}\left(r\frac{\partial c}{\partial r}\right) + \frac{1}{r^2}\frac{\partial^2 c}{\partial \theta^2}\right]. \tag{8}$$

The boundary conditions on the inner cylinder become

$$c_r = 0 \quad \text{and} \quad w = 0 \quad \text{on} \quad r = a \tag{9}$$

and the boundary conditions on the outer cylinder become

$$c = \begin{cases} c_0 & \text{for} \quad 0 \le \theta < \pi \\ 0 & \text{for} \quad \pi \le \theta < 2\pi \end{cases} \quad \text{and} \quad w = w_0 \quad \text{on} \quad r = b. \tag{10}$$

Clearly this problem is periodic in θ, i.e.

$$c(r,\theta) = c(r,\theta+2\pi) \quad \text{and} \quad p(r,\theta) = p(r,\theta+2\pi).$$

For the pressure to be periodic and satisfy equation (6) requires that $\frac{\partial p}{\partial \theta} = 0$. Thus equation (7) can be analytically solved to give

$$w = \frac{A}{r} + Br$$

and using the boundary conditions (9) and (10) we can solve for A and B to determine that

$$w = \frac{bw_0(r^2 - a^2)}{r(b^2 - a^2)}. \tag{11}$$

The problem has now been reduced to solving the mass transport equation (8) where w is given in equation (11).

2.1. Non-dimensionalisation

We non-dimensionalise the system by rescaling the variables as follows:

$$\theta = \pi\tau, \quad r = bR, \quad c = c_0 C$$

and define the Péclet number and the ratio of the radii of the cylinders as

$$\mathrm{Pe} = \frac{bw_0}{\pi D} \quad \text{and} \quad \kappa = \frac{a}{b}.$$

Then the dimensionless mass transport equation can be written as

$$\mathrm{Pe}\left(\frac{R^2 - \kappa^2}{1 - \kappa^2}\right)C_\tau = RC_R + R^2C_{RR} + \pi^{-2}C_{\tau\tau} \quad \text{for} \quad \kappa < R < 1. \tag{12}$$

The boundary condition on the inner cylinder becomes

$$C_R = 0 \quad \text{on} \quad R = \kappa \tag{13}$$

and the boundary condition on the outer cylinder becomes

$$C = \begin{cases} 1 & \text{for} \quad 0 \le \tau < 1 \\ 0 & \text{for} \quad 1 \le \tau < 2 \end{cases} \quad \text{on} \quad R = 1. \tag{14}$$

2.2. Effective diffusivity

Let f denote the dimensional flux on the upper half of the cylinder, then

$$f = -\frac{D}{\pi}\int_0^{\pi} c_r|_{r=b}\, d\theta.$$

The effective diffusivity can be defined as

$$D_{\text{eff}} = -\frac{f}{\bar{c}_r} = \frac{bD}{\pi c_0}\int_0^{\pi} c_r|_{r=b}\, d\theta = D\int_0^{1} C_R|_{R=1}\, d\tau \tag{15}$$

where $\bar{c}_r$ is the mean macroscopic gradient, here we use $\bar{c}_r = c_0/b$.

2.3. Small Péclet number limit

In the small Péclet number limit, the leading order term can be obtained by setting $\text{Pe} = 0$, then the problem can be solved using separation of variables to give

$$C(R,\tau) = \frac{1}{2} + \frac{2}{\pi}\sum_{m=1}^{\infty}\frac{R^{2m-1} + \kappa^{4m-2}R^{1-2m}}{(2m-1)(1+\kappa^{4m-2})}\sin((2m-1)\pi\tau). \tag{16}$$

Notice, if we substitute equation (16) into equation (15) we obtain

$$D_{\text{eff}} = \frac{4D}{\pi^2}\sum_{m=1}^{\infty}\frac{1-\kappa^{4m-2}}{(1+\kappa^{4m-2})(2m-1)}$$

which is not a convergent series. This unlikely result may be due to taking the derivatives of the infinite series in equation (16), and so an alternative version of the solution may yield a finite value for the effective diffusivity.

3. Large Péclet number limit

In the large Péclet number limit, there is a concentration boundary layer of thickness of $\text{Pe}^{-\frac{1}{2}}$ near the outer cylinder. Outside of this boundary layer the concentration becomes homogeneous. We introduce the boundary layer coordinate

$$\sigma = \sqrt{\text{Pe}}(1-R) \tag{17}$$

then equation (12) becomes

$$\left(\text{Pe} - \frac{2\sigma\sqrt{\text{Pe}} - \sigma^2}{1-\kappa^2}\right)C_\tau - (\sqrt{\text{Pe}} - \sigma)^2 C_{\sigma\sigma} = \frac{C_{\tau\tau}}{\pi^2} - (\sqrt{\text{Pe}} - \sigma)C_\sigma \tag{18}$$

for $0 < \sigma < \sqrt{\text{Pe}}(1-\kappa)$. We now introduce the expansion

$$C = C^0 + \text{Pe}^{-1/2}C^1 + O(\text{Pe}^{-1}).$$

Substituting this into the above equations, letting the Péclet number tend to infinity, and collecting powers of Pe yields

$$C^0_\tau = C^0_{\sigma\sigma}, \tag{19}$$

$$C^1_\tau = C^1_{\sigma\sigma} + \phi\sigma C^0_{\sigma\sigma} - C^0_\sigma \quad \text{where} \quad \phi = \frac{2\kappa^2}{1-\kappa^2} \tag{20}$$

for $0 < \sigma < \infty$. Now the boundary conditions become

$$C^0_\sigma, C^1_\sigma, \to 0 \quad \text{as} \quad \sigma \to \infty$$

and

$$C^0 = \begin{cases} 1 & \text{for} \quad 0 \le \tau < 1 \\ 0 & \text{for} \quad 1 \le \tau < 2 \end{cases} \quad \text{and} \quad C^1 = 0 \quad \text{on} \quad \sigma = 0. \tag{21}$$

As the problem is periodic in τ with a period of 2, the concentration must tend to a constant as σ tends to infinity. Hence, using symmetry we obtain

$$C^0(\sigma,\tau) = 1 - C^0(\sigma,\tau+1), \quad C^1(\sigma,\tau) = -C^1(\sigma,\tau+1), \tag{22}$$

which are the global self-consistency conditions. As $C^0(\sigma,\tau)$ tends to a constant as σ tends to infinity, if we call this constant Θ and use equation (22) we obtain $\Theta = 1 - \Theta$, hence, $\Theta = \frac{1}{2}$, thus we can write our far field boundary conditions as

$$C^0 \to \frac{1}{2} \quad \text{and} \quad C^1 \to 0 \quad \text{as} \quad \sigma \to \infty. \tag{23}$$

4. Zeroth order

We are going to solve this problem using the Fourier sine transformation, however, in order to use this we need homogeneous boundary conditions. We now seek a self-similar solution $\overline{C}(\sigma,\tau)$ in the upper half of the domain, i.e. for $0 \le \tau \le 1$. We seek a solution that satisfies

$$\overline{C}_\tau = \overline{C}_{\sigma\sigma} \quad \text{for} \quad 0 < \sigma < \infty \tag{24}$$

with the inhomogeneous boundary conditions

$$\overline{C} \to \frac{1}{2} \quad \text{as} \quad \sigma \to \infty \quad \text{and} \quad \overline{C} = 1 \quad \text{on} \quad \sigma = 0. \tag{25}$$

The self-similar solution to this problem is given by

$$\overline{C} = 1 - \frac{1}{2}\text{erf}\left(\frac{\sigma}{2\sqrt{\tau}}\right). \tag{26}$$

Then we construct the homogeneous part of the zeroth order in the upper half of the domain using

$$C^0 = \overline{C} + \hat{C}$$

where $\hat{C}$ satisfies

$$\hat{C}_\tau = \hat{C}_{\sigma\sigma} \quad \text{for} \quad 0 < \sigma < \infty \tag{27}$$

with the homogeneous boundary conditions

$$\hat{C} \to 0 \quad \text{as} \quad \sigma \to \infty \quad \text{and} \quad \hat{C} = 0 \quad \text{on} \quad \sigma = 0. \tag{28}$$

Using the global self consistency condition (22) with the self similar solution (26) we obtain

$$\hat{C}(\sigma,0) = \frac{1}{2}\text{erf}\left(\frac{\sigma}{2}\right) - \frac{1}{2} - \hat{C}(\sigma,1). \tag{29}$$

By taking the Fourier sine transform, given in Appendix A, of (27) and solving we obtain

$$U^0(k,\tau) = G^0(k)e^{-k^2\tau} \tag{30}$$

where $U^0 = \mathcal{F}^s\{\hat{C}\}$ and $G^0(k)$ needs to be determined. Taking the Fourier sine transform of the global self consistency condition (29) yields

$$U^0(k,0) = \mathcal{F}^s\left\{\frac{1}{2}\text{erf}\left(\frac{\sigma}{2}\right) - \frac{1}{2}\right\} - U^0(k,1). \tag{31}$$

Now

$$\mathcal{F}^s\left\{\text{erf}\left(\frac{\sigma}{2}\right) - 1\right\} = \sqrt{\frac{2}{\pi}}\int_0^{\infty}\left(\text{erf}\left(\frac{\sigma}{2}\right) - 1\right)\sin(k\sigma)d\sigma = \sqrt{\frac{2}{\pi}}\frac{e^{-k^2} - 1}{k}. \tag{32}$$

Substituting equations (30) and (32) into equation (31) allows $G^0(k)$ to be obtained. Hence, we can obtain the solution

$$U^0(k,\tau) = \frac{e^{-k^2\tau}(e^{-k^2} - 1)}{\sqrt{2\pi}k(e^{-k^2} + 1)}. \tag{33}$$

Taking the inverse Fourier sine transform of equation (33) yields

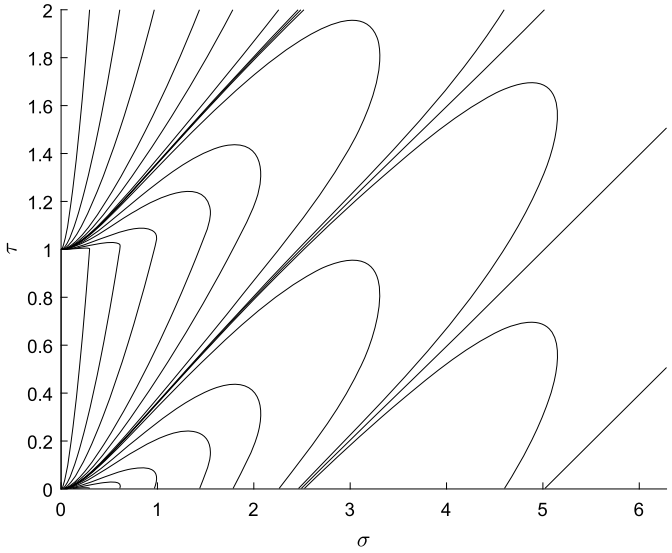

Fig. 1. Contours of C^0 in the $\sigma-\tau$ plane using equations (35) and (36).

$$\hat{C}=\sqrt{\frac{2}{\pi}}\int_0^\infty U^0(k,\tau)\sin(k\sigma)\,dk=\int_0^\infty \frac{e^{-k^2\tau}(e^{-k^2}-1)}{\pi k(e^{-k^2}+1)}\sin(k\sigma)\,dk. \quad (34)$$

Combining the homogeneous and inhomogeneous solutions yield

$$C^0=\overline{C}+\hat{C}=1-\frac{1}{2}\mathrm{erf}\left(\frac{\sigma}{2\sqrt{\tau}}\right)+\int_0^\infty \frac{e^{-k^2\tau}(e^{-k^2}-1)}{\pi k(e^{-k^2}+1)}\sin(k\sigma)\,dk.$$

Using this result

$$\int_0^\infty \frac{e^{-k^2\tau}}{\pi k}\sin(k\sigma)\,dk=\frac{1}{2}\mathrm{erf}\left(\frac{\sigma}{2\sqrt{\tau}}\right)$$

we can express the zeroth order solution in the upper half of the domain as

$$C^0(\sigma,\tau)=1-\frac{2}{\pi}\int_0^\infty \frac{e^{-k^2\tau}\sin(k\sigma)}{k(e^{-k^2}+1)}\,dk \quad \text{for} \quad 0\le\tau\le 1, \quad \sigma\ge 0. \quad (35)$$

Using the zeroth order solution in the upper half of the domain, we can obtain the zeroth order solution in the lower half of the domain using $C^0(\sigma,\tau+1)=1-C^0(\sigma,\tau)$ to give

$$C^0(\sigma,\tau)=\frac{2}{\pi}\int_0^\infty \frac{e^{-k^2(\tau-1)}\sin(k\sigma)}{k(e^{-k^2}+1)}\,dk \quad \text{for} \quad 1\le\tau\le 2, \quad \sigma\ge 0. \quad (36)$$

Using Simpsons' rule we numerically evaluated these integrals and in Fig. 1 we illustrate contours of the concentration C^0 in the $\sigma-\tau$ plane. In Fig. 1, for small values of σ, we see contours almost parallel to the τ-axis, except near $\tau=0$, 1 and 2 which show contours clustering together denoting a large change in concentration. The contours of $C^0=\frac{1}{2}$ are approximately lines parallel to $\tau=\sigma/\pi$ separated by 1 in τ. We observe that for large σ that C^0 tends $\frac{1}{2}$.

5. First order

Taking the Fourier sine transform of the first order equation in (20) and solving yields

$$U^1(k,\tau)=e^{-k^2\tau}\left(\int_0^\tau e^{k^2z}E^1\,dz+G^1(k)\right)$$

where $U^1(k,\tau)=\mathcal{F}^s\left\{C^1(\sigma,\tau)\right\}$, $G^1(k)$ is an arbitrary function and

$$\begin{aligned}E^1(k,z)&=\mathcal{F}^s\left\{\phi\sigma C^0_{\sigma\sigma}(\sigma,z)-C^0_\sigma(\sigma,z)\right\}\\&=\sqrt{\frac{2}{\pi}}\int_0^\infty(\phi\sigma C^0_{\sigma\sigma}(\sigma,z)-C^0_\sigma(\sigma,z))\sin(k\sigma)\,d\sigma\\&=\frac{2^{3/2}}{\pi^{3/2}}\int_0^\infty\int_0^\infty\frac{e^{-\lambda^2z}\sin(k\sigma)}{e^{-\lambda^2}+1}(\phi\sigma\lambda\sin(\lambda\sigma)+\cos(\lambda\sigma))\,d\lambda d\sigma. \quad (37)\end{aligned}$$

Taking the Fourier sine transform of the global self consistency condition (22) yields $U^1(k,0)=-U^1(k,1)$, thus we can solve for G^1 to obtain

$$U^1(k,\tau)=\frac{e^{-k^2\tau}}{1+e^{-k^2}}\left(\int_0^\tau e^{k^2z}E^1\,dz-\int_\tau^1 e^{k^2(z-1)}E^1\,dz\right). \quad (38)$$

Taking the inverse Fourier sine transform of equation (38) yields

$$\begin{aligned}C^1&=\sqrt{\frac{2}{\pi}}\int_0^\infty U^1(k,\tau)\sin(k\sigma)\,dk\\&=\sqrt{\frac{2}{\pi}}\int_0^\infty\frac{e^{-k^2\tau}}{1+e^{-k^2}}\left(\int_0^\tau e^{k^2z}E^1\,dz-\int_\tau^1 e^{k^2(z-1)}E^1\,dz\right)\sin(k\sigma)\,dk. \quad (39)\end{aligned}$$

If we substitute in the expression for E^1 given in equation (37) into equation (39) and evaluate the integral in z we obtain

$$C^1(\sigma,\tau)=\frac{4}{\pi^2}\int_0^\infty\int_0^\infty\int_0^\infty\Lambda\,d\lambda d\chi\sin(k\sigma)\,dk \quad (40)$$

where

$$\Lambda=\left(\frac{e^{-\lambda^2\tau}}{1+e^{-\lambda^2}}-\frac{e^{-k^2\tau}}{1+e^{-k^2}}\right)\frac{\phi\chi\lambda\sin(\lambda\chi)+\cos(\lambda\chi)}{k^2-\lambda^2}\sin(k\chi). \quad (41)$$

Hence, we have obtained C^1 which is the first order correction to C^0. Using this correction we can obtain a more accurate approximation to the effective diffusivity in the large Péclet number limit.

6. Effective diffusivity

To obtain the effective diffusivity in the large Péclet number limit we can use the boundary layer coordinate to obtain

$$D_{\mathrm{eff}}=-D\sqrt{\mathrm{Pe}}\int_0^1 C_\sigma|_{\sigma=0}\,d\tau=D\sqrt{\mathrm{Pe}}I \quad (42)$$

with $I=I^0+\mathrm{Pe}^{-1/2}I^1+O(\mathrm{Pe}^{-1})$, where O is the upper bound used in asymptotic analysis, and

$$I^0=-\int_0^1 C^0_\sigma|_{\sigma=0}\,d\tau \quad \text{and} \quad I^1=-\int_0^1 C^1_\sigma|_{\sigma=0}\,d\tau. \quad (43)$$

6.1. Zeroth order term

Using C^0 given in equation (35) we find that

$$I^0=\frac{2}{\pi}\int_0^\infty\Delta\,dk=\frac{1}{\pi}\int_{-\infty}^\infty\Delta\,dk \quad \text{where} \quad \Delta=\frac{1-e^{-k^2}}{k^2(e^{-k^2}+1)}$$

which has been converted into an integral across the whole real line. By converting I^0 into a contour integral around a semi-circle in the upper half of the complex plane centred at $k=0$ and noting that the integral around the arc tends to zero as the radius of the arc tends to infinity, we can evaluate I^0 using Cauchy's residue theorem:

$$\int_\Gamma \frac{f(z)}{z-z_0}\,dz = 2\pi i f(z_0)$$

where Γ is a closed contour containing the pole at $z = z_0$. For each simple pole we can use

$$\int_\Gamma \frac{\psi(z)}{\eta(z)}\,dz = 2\pi i \frac{\psi(z_0)}{\eta'(z_0)}$$

where $\eta(z)$ has a simple zero at $z = z_0$, so $\eta'(z_0) \neq 0$. Notice that $\Delta(0) = \frac{1}{2}$ so Δ is not singular at $k = 0$, hence all the poles of Δ occur at the solutions to $e^{-k^2} + 1 = 0$. The roots of $e^{-k^2} + 1 = 0$ in the upper half of the complex plane are at $k = \alpha_n$ and $k = \beta_n$ for $n \geq 0$ where

$$\alpha_n = \sqrt{\pi\left(n+\frac{1}{2}\right)}(i-1) \quad \text{and} \quad \beta_n = \sqrt{\pi\left(n+\frac{1}{2}\right)}(i+1).$$

Hence, we obtain

$$\begin{aligned} I^0 &= 2i\sum_{n=0}^{\infty} \text{Residue}\left(\Delta, k=\alpha_n\right) + 2i\sum_{n=0}^{\infty} \text{Residue}\left(\Delta, k=\beta_n\right) \\ &= 2i\sum_{n=0}^{\infty}\alpha_n^{-3} + 2i\sum_{n=0}^{\infty}\beta_n^{-3} = \frac{\sqrt{2}}{\pi^{3/2}}\left(\sum_{n=0}^{\infty}\frac{1+i}{(2n+1)^{3/2}} + \sum_{n=0}^{\infty}\frac{1-i}{(2n+1)^{3/2}}\right) \\ &= \frac{2^{3/2}}{\pi^{3/2}}\sum_{n=0}^{\infty}(2n+1)^{-3/2} = \frac{2^{3/2}}{\pi^{3/2}}\left(\sum_{n=1}^{\infty}n^{-3/2} - \sum_{n=1}^{\infty}(2n)^{-3/2}\right) \\ &= \frac{2^{3/2}(1-2^{-3/2})}{\pi^{3/2}}\sum_{n=1}^{\infty}n^{-3/2} = \frac{2^{3/2}-1}{\pi^{3/2}}\zeta\left(\frac{3}{2}\right) \approx 0.85780470 \end{aligned} \tag{44}$$

using $\zeta\left(\frac{3}{2}\right) = \sum_{n=1}^{\infty} n^{-3/2} \approx 2.61237535$ where ζ is the Riemann-zeta function (Abramowitz and Stegun, 1968).

6.2. First order term

Using C^1 given in equation (40) we find that

$$I^1 = -\frac{4}{\pi^2}\int_0^1\int_0^\infty\int_0^\infty\int_0^\infty \Lambda k\; d\lambda d\chi dk d\tau.$$

We now evaluate the integral in τ to obtain

$$I^1 = \frac{4}{\pi^2}\int_0^\infty\int_0^\infty\int_0^\infty (\phi\lambda\chi\sin(\lambda\chi) + \cos(\lambda\chi))\Omega\sin(k\chi)\; d\lambda d\chi dk$$

where

$$\Omega = \frac{(k^2-\lambda^2)(e^{-k^2-\lambda^2}-1) + (k^2+\lambda^2)(e^{-\lambda^2}-e^{-k^2})}{k\lambda^2(k^2-\lambda^2)(1+e^{-k^2})(1+e^{-\lambda^2})}. \tag{45}$$

Notice that Ω is not singular at $k = 0$, $\lambda = 0$ or $k = \lambda$. To allow us to approximate this triple integral we shall introduce I_L^1 where we have truncated the domain size to $[0, L]$ in each dimension, and hence

$$I_L^1 = \frac{4}{\pi^2}\int_0^L\int_0^L\int_0^L (\phi\lambda\chi\sin(\lambda\chi) + \cos(\lambda\chi))\Omega\sin(k\chi)\; d\lambda d\chi dk$$

and then we analytically evaluate the integral with respect to χ to obtain

$$I_L^1 = J_L^0 + \phi J_L^1 \tag{46}$$

with

$$J_L^0 = \frac{2}{\pi^2}\int_0^L\int_0^L \Omega P_0\; d\lambda dk \quad \text{and} \quad J_L^1 = \frac{2}{\pi^2}\int_0^L\int_0^L \lambda\Omega(LP_1 + P_2)\; d\lambda dk$$

Table 1
J_L^0 and J_L^1 as a function of the domain size L.

L	J_L^0	J_L^1
10	−0.1975622244	−0.1342850967
20	−0.2232219954	−0.1281002227
40	−0.2364765293	−0.1259596249
80	−0.2432057528	−0.1252849260
160	−0.2465948546	−0.1250823458
320	−0.2482954350	−0.1250233477
640	−0.2491472139	−0.1250065255
1280	−0.2495734117	−0.1250018058

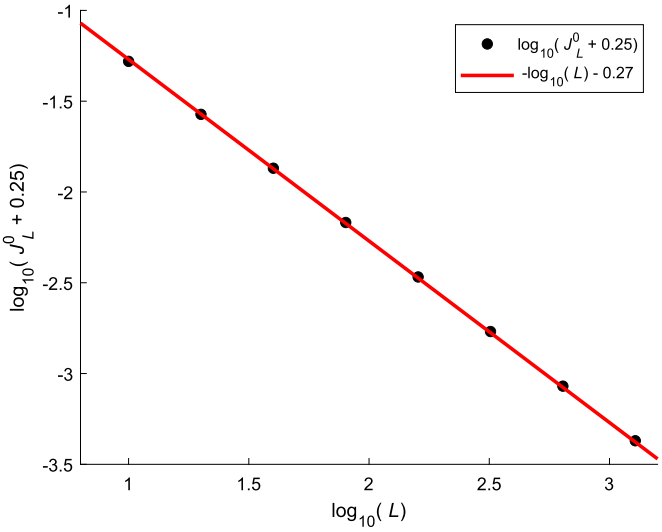

Fig. 2. $\log_{10}(J_L^0+0.25)$ against $\log_{10}(L)$ using the values in Table 1. Additionally the red line corresponds to the line of best fit.

where

$$P_0 = \frac{\cos(L(\lambda-k))}{\lambda-k} - \frac{\cos(L(\lambda+k))}{\lambda+k} - \frac{2k}{\lambda^2-k^2},$$
$$P_1 = \frac{\sin(L(\lambda-k))}{\lambda-k} - \frac{\sin(L(\lambda+k))}{\lambda+k},$$
$$P_2 = \frac{\cos(L(\lambda-k))}{(\lambda-k)^2} - \frac{\cos(L(\lambda+k))}{(\lambda+k)^2} - \frac{4\lambda k}{(\lambda^2-k^2)^2}.$$

We numerically evaluated the double integrals in equation (46) using Simpsons rule. In Table 1 we present the numerically evaluated values of J_L^0 and J_L^1 for various domain sizes L. The double integrals were numerically evaluated using a spatial step of 0.0025 in each dimension. Fig. 2 illustrates $\log_{10}(J_L^0+0.25)$ against $\log_{10}(L)$. The line of best fit in Fig. 2 suggests the relationship

$$J_L^0 = -\frac{1}{4} + \frac{0.537}{L}.$$

Thus as L tends to infinity we expect that $J^0 = -\frac{1}{4}$. Fig. 3 illustrates $\log_{10}(-J_L^1-0.125)$ against $\log_{10}(L)$. The line of best fit in Fig. 3 suggests the relationship

$$J_L^1 = -\frac{1}{8} - \frac{0.562}{L^{1.75}}.$$

Thus as L tends to infinity we expect that $J^1 = -\frac{1}{8}$. Substituting these predicted values of J^0 and J^1 into I^1 yields

$$I^1 = -\frac{1}{4} - \frac{\phi}{8}. \tag{47}$$

Substituting this conjecture into the effective diffusivity equation (42) yields

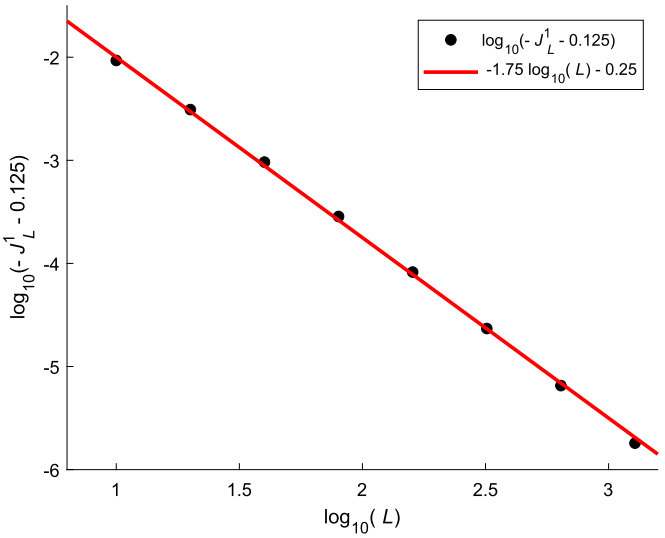

Fig. 3. $\log_{10}(-J_L^1 - 0.125)$ against $\log_{10}(L)$ using the values in Table 1. Additionally the red line corresponds to the line of best fit.

Table 2
Numerical values of I_{num} as a function of Pe when $\kappa = 1/2$, obtained from the full problem on various meshes N with $M = \lambda N$.

I_{num}		N				
Pe	λ	200	400	800	1600	3200
100	5	0.7948	0.8125	0.8292	0.8450	0.8601
250	12.5	0.8223	0.8298	0.8387	0.8481	0.8573
500	25	0.8358	0.8386	0.8430	0.8488	0.8548
1000	50	0.8432	0.8448	0.8465	0.8493	0.8525
2500	125	0.8465	0.8495	0.8505	0.8508	/
5000	250	0.8449	0.8508	0.8524	/	/

$$\frac{D_{\text{eff}}}{D\sqrt{\text{Pe}}} = \frac{2^{3/2}-1}{\pi^{3/2}}\zeta\left(\frac{3}{2}\right) - \frac{2+\phi}{8\sqrt{\text{Pe}}} + O(\text{Pe}^{-1})$$
$$\approx 0.8578047 - \frac{2+\phi}{8\sqrt{\text{Pe}}} + O(\text{Pe}^{-1}). \tag{48}$$

We note that increasing the ratio κ, increases ϕ which decreases the effective diffusivity.

7. Numerical solutions

To verify this large Péclet asymptotic limit we numerically solved equation (18) by discretizing it using second order finite differences. For convenience we choose $\kappa = \frac{1}{2}$. We used periodic boundary conditions in τ, namely $C(\sigma, 0) = C(\sigma, 2)$. On the outer cylinder, $\sigma = 0$, we used boundary condition (14) and on the inner cylinder, when $\sigma = \sqrt{\text{Pe}}(1-\kappa)$ we used $C_\sigma = 0$. In the σ direction we used N mesh points and in the τ direction we used M mesh points. To ensure that C remained between 0 and 1 we choose $M = \lambda N$ where $\lambda = \text{Pe}/20$. This condition was only required for large values of Pe. Using equation (42) we have

$$I = \frac{D_{\text{eff}}}{D\sqrt{\text{Pe}}} = -\int_0^1 C_\sigma|_{\sigma=0}\, d\tau.$$

As C will now be obtained numerically, we introduce I_{num} to denote our numerical approximation to the value of I. The system of equations were solved by iterating until the value of I_{num} had converged to 4 decimal places. In Table 2 we present the values of I_{num} as a function of the Péclet number for a range of meshes. Table 2 shows that the value of I_{num} appears to be converging for large values of Pe, however, for moderate values of Pe, the values do not appear to have finished converging, over the range of meshes considered. The 3 missing values in Table 2 were due to meshes requiring more memory than our Fortran compiler would allow.

Table 3
Comparing I_{num} (on finest mesh in Table 2) with I_{asy} (equation (49)) for $\kappa = 1/2$ for selected values of Pe. Error $= |I_{\text{num}} - I_{\text{asy}}|/I_{\text{num}}$.

Pe	N	M	I_{num}	I_{asy}	Error
100	3200	16000	0.8601	0.8245	4.14%
250	3200	40000	0.8573	0.8367	2.46%
500	3200	80000	0.8548	0.8429	1.39%
1000	3200	160000	0.8525	0.8473	0.61%
2500	1600	200000	0.8508	0.8511	0.04%
5000	800	200000	0.8524	0.8531	0.08%

When $\kappa = \frac{1}{2}$ this means that $\phi = \frac{2}{3}$, so the large Péclet number asymptotic prediction of the effective diffusivity in equation (48) yields

$$I_{\text{asy}} = \frac{D_{\text{eff}}}{D\sqrt{\text{Pe}}} = 0.8578047 - \frac{1}{3\sqrt{\text{Pe}}} + O(\text{Pe}^{-1}) \tag{49}$$

where I_{asy} is the predicted asymptotic value of I in the large Pe limit. In Table 3 we compare the asymptotic value I_{asy} given by equation (49) with the value I_{num} obtained from the full numerical problem on the finest mesh considered for each value of Pe. The last column in Table 3 is the percentage error of the asymptotic solution with the full numerical solution I_{num}. Table 3 shows that the numerical I_{num} and asymptotic I_{asy} values are in very good for large values of Pe, say around 2500, however, as Pe decreases the numerical and asymptotic values have the opposite trend. The numerical values tend to increase as Pe decreases, however, the asymptotic values decrease as Pe decreases. One possible cause of this divergence in the results could be that the next correction in the series, a $O(\text{Pe}^{-1})$ term not obtained here, may become more important than the $O(\text{Pe}^{-1/2})$ term obtained here.

In section 2.3 we found that the small Pe limit yields an infinite value of D_{eff} whilst the large Pe limit predicted I_{asy} to be an increasing function of Pe, hence, we should expect a minimum in I from the two asymptotic limits. Overall, there is good agreement in the predicted effective diffusivity in the large Péclet number limit with the results from the full solution for $\kappa = \frac{1}{2}$.

8. Conclusions

In this study we have analysed mass transport in Couette flow. In the large Péclet number limit, using the Fourier sine transform, the asymptotic concentration profile in the boundary layer has been obtained as an integral solution. The asymptotic solution agrees well with the full numerical solution for large Péclet numbers. Further, the analytical asymptotic prediction in the large Péclet number limit of the effective diffusivity is in good agreement with those obtained by full numerical solutions, for large values of Pe. To demonstrate the application of the approach used, in Appendix B, the same analysis is applied to planar Couette flow when a periodic concentration is specified on a moving wall and the effective diffusivity is obtained in the large Péclet number limit.

CRediT authorship contribution statement

A.S. Hamilton-Morris: Validation, Software, Investigation. **S.C. Generalis:** Writing – review & editing. **P.T. Griffiths:** Writing – review & editing. **P.M.J. Trevelyan:** Formal analysis, Conceptualization, Investigation, Methodology, Project administration, Software, Supervision, Validation, Visualization, Writing – original draft, Writing – review & editing.

Declaration of competing interest

The authors declare that they have no known competing financial interests or personal relationships that could have appeared to influence the work reported in this paper.

Data availability

Data will be made available on request.

Acknowledgements

The authors would like to thank Prof. Anne De Wit for many useful discussions.

Appendix A. Fourier sine transform

The Fourier sine transform is defined by

$$\mathcal{F}^s\{q(\sigma)\} = \sqrt{\frac{2}{\pi}} \int_0^\infty q(\sigma)\sin(k\sigma)\, d\sigma = Q(k) \tag{50}$$

$$(\mathcal{F}^s)^{-1}\{Q(k)\} = \sqrt{\frac{2}{\pi}} \int_0^\infty Q(k)\sin(k\sigma)\, dk = q(\sigma). \tag{51}$$

We require that q and q_σ tend to zero as σ tends to infinity, then we have the property

$$\mathcal{F}^s\{q_{\sigma\sigma}\} = \sqrt{\frac{2}{\pi}} kq(0) - k^2\mathcal{F}^s\{q(\sigma)\}. \tag{52}$$

Appendix B. Planar Couette flow

Suppose we now have two horizontal parallel plates. The x axis runs horizontally parallel to the plates whilst the y axis runs vertically perpendicular to the plates. The lower plate is at $y = 0$ at moves to the right at speed u_0, whilst the upper plate at $y = h$ is stationary. We suppose a fluid is between the two plates with constant density ρ and kinematic viscosity ν. We assume that the fluid satisfies the incompressible Navier-Stokes equations. A species C with molecular diffusion coefficient D will dissolve into the fluid. We assume that the concentration is sufficiently dilute that saturation effects can be neglected so that the concentration c satisfies the mass transport equation. We assume that the species does not affect the density or viscosity of the fluid, hence we have the bulk equations:

$$\underline{\nabla}\cdot\underline{u} = 0, \tag{53}$$

$$\underline{u}_t + (\underline{u}\cdot\underline{\nabla})\underline{u} = -\frac{1}{\rho}\underline{\nabla}p + \nu\nabla^2\underline{u}, \tag{54}$$

$$c_t + (\underline{u}\cdot\underline{\nabla})c = D\nabla^2 c \tag{55}$$

where $\underline{u}$ is the fluids velocity, p is the fluid's pressure and t is time. We suppose the upper plate is impermeable so that we have the no slip and no flux boundary conditions:

$$c_y = 0 \quad \text{and} \quad \underline{u} = \underline{0} \quad \text{on} \quad y = h. \tag{56}$$

The lower plate is assumed permeable. We suppose that there is a set of large containers, below the lower plate. Each container is fixed in space and of equal width w. The contents of the containers periodically alternate between containing species C at the concentration c_0 for $0 \le x < w$, or containing a large amount of catalyst such that when species C makes contact with the catalyst it undergoes a first order chemical reaction for $w \le x < 2w$. We suppose that the reaction rate of the chemical reaction is sufficiently fast that it can be assumed instantaneous. Thus, on the lower plate we shall assume that species C is held at a constant concentration c_0 for $0 \le x < w$, but C is absent for $w \le x < 2w$, and the problem has period $2w$ in the x direction. Hence, on the lower plate we have the boundary conditions:

$$c = \begin{cases} c_0 & \text{for} \quad 0 \le x < w \\ 0 & \text{for} \quad w \le x < 2w \end{cases} \quad \text{and} \quad \underline{u} = u_0\underline{i} \quad \text{on} \quad y = 0 \tag{57}$$

where $\underline{i}$ is the unit vector in the x direction. We assume that the flow and concentration have reached a steady state, i.e. $c_t = 0$ and $\underline{u}_t = \underline{0}$. Further, we assume that the flow field is purely in the x direction and so takes the form $\underline{u} = u(y)\underline{i}$. Then the incompressibility condition is already satisfied and the bulk equations become

$$0 = -\frac{1}{\rho}\frac{\partial p}{\partial x} + \nu u_{yy}, \tag{58}$$

$$0 = -\frac{1}{\rho}\frac{\partial p}{\partial y}, \tag{59}$$

$$u\frac{\partial c}{\partial x} = D\left[\frac{\partial^2 c}{\partial x^2} + \frac{\partial^2 c}{\partial y^2}\right]. \tag{60}$$

The boundary conditions on the upper plate become

$$c_y = 0 \quad \text{and} \quad u = 0 \quad \text{on} \quad y = h \tag{61}$$

and the boundary conditions on the lower plate become

$$c = \begin{cases} c_0 & \text{for} \quad 0 \le x < w \\ 0 & \text{for} \quad w \le x < 2w \end{cases} \quad \text{and} \quad u = u_0 \quad \text{on} \quad y = 0. \tag{62}$$

This problem is periodic in x, i.e.

$$c(x, y) = c(x + 2w, y) \quad \text{and} \quad \frac{\partial p}{dx}(x, y) = \frac{\partial p}{dx}(x + 2w, y).$$

Now from equation (59) we see that p is only a function of x. We suppose that this problem involves a constant pressure gradient in the x direction, i.e. $\frac{dp}{dx}$ is a constant. Solving equation (58) yields

$$u = \frac{y^2}{2\mu}\frac{dp}{dx} + Ay + B$$

where $\mu = \rho\nu$ is the dynamic viscosity, and A and B are constants. Using the boundary conditions (61) and (62) we can solve for A and B to determine that

$$u = (h - y)\left(\frac{u_0}{h} - \frac{y}{2\mu}\frac{dp}{dx}\right). \tag{63}$$

Non-dimensionalisation

We non-dimensionalise the system by rescaling the variables as follows:

$$x = w\tau, \quad y = hY, \quad c = c_0 C, \quad p = \frac{2w\mu u_0}{h^2}P$$

and define the Péclet number as

$$\mathrm{Pe} = \frac{h^2 u_0}{wD}.$$

Then the dimensionless mass transport equation can be written as

$$\mathrm{Pe}\,(1 - Y)(1 - P_\tau Y)C_\tau = C_{YY} + \frac{h^2}{w^2}C_{\tau\tau} \quad \text{for} \quad 0 < Y < 1. \tag{64}$$

The boundary condition on the upper plate becomes

$$C_Y = 0 \quad \text{on} \quad Y = 1 \tag{65}$$

and the boundary condition on the lower plate becomes

$$C = \begin{cases} 1 & \text{for} \quad 0 \le \tau < 1 \\ 0 & \text{for} \quad 1 \le \tau < 2 \end{cases} \quad \text{on} \quad Y = 0. \tag{66}$$

Effective diffusivity

Let f denote the dimensional flux on the lower plate, then

$$f = -\frac{D}{w}\int_0^w c_y|_{y=0}\, dx.$$

The effective diffusivity can be defined as

$$D_{\text{eff}} = -\frac{f}{\bar{c}_y} = \frac{hD}{wc_0}\int_0^w c_y|_{y=0}\, dx = D\int_0^1 C_Y|_{Y=0}\, d\tau \tag{67}$$

where $\bar{c}_y$ is the mean macroscopic gradient, here we use $\bar{c}_y = c_0/h$.

Small Péclet number limit

In the small Péclet number limit, setting $\text{Pe} = 0$ allows the problem to be solved using separation of variables to give

$$C(Y,\tau) = \frac{1}{2} + \frac{2}{\pi}\sum_{m=1}^{\infty}\frac{\cosh((2m-1)\frac{\pi h}{w}(1-Y))}{\cosh((2m-1)\frac{\pi h}{w})}\frac{\sin((2m-1)\pi\tau)}{2m-1}. \tag{68}$$

We notice we cannot use this solution to obtain the effective diffusivity, since if we substitute equation (68) into equation (67) we obtain

$$D_{\text{eff}} = -\frac{4Dh}{w\pi}\sum_{m=1}^{\infty}\frac{\tanh((2m-1)\frac{\pi h}{w})}{2m-1}$$

which is not a convergent series.

A Large Péclet number limit

In the large Péclet number limit, there is a concentration boundary layer of thickness of $\text{Pe}^{-\frac{1}{2}}$ near the lower plate. Outside of this boundary layer the concentration becomes homogeneous. We introduce the boundary layer coordinate

$$\sigma = \sqrt{\text{Pe}}Y \tag{69}$$

then equation (64) becomes

$$\left(1-\frac{\sigma}{\sqrt{\text{Pe}}}\right)\left(1-P_\tau\frac{\sigma}{\sqrt{\text{Pe}}}\right)C_\tau = \frac{h^2}{w^2\text{Pe}}C_{\tau\tau} + C_{\sigma\sigma} \tag{70}$$

for $0 < \sigma < \sqrt{\text{Pe}}$. We now introduce the expansion

$$C = C^0 + \text{Pe}^{-1/2}C^1 + O(\text{Pe}^{-1}).$$

Substituting this into the above equations, letting the Péclet number tend to infinity, and collecting powers of Pe yields

$$C^0_\tau = C^0_{\sigma\sigma}, \tag{71}$$

$$C^1_\tau = C^1_{\sigma\sigma} + (1+P_\tau)\sigma C^0_{\sigma\sigma}, \tag{72}$$

for $0 < \sigma < \infty$. Now the boundary conditions become

$$C^0_\sigma, C^1_\sigma \to 0 \quad \text{as} \quad \sigma \to \infty$$

and

$$C^0 = \begin{cases} 1 & \text{for} \quad 0 \le \tau < 1 \\ 0 & \text{for} \quad 1 \le \tau < 2 \end{cases} \quad \text{and} \quad C^1 = 0 \quad \text{on} \quad \sigma = 0.$$

As the problem is periodic in τ with a period of 2, the concentration must tend to a constant as σ tends to infinity. Hence, using symmetry we obtain

$$C^0(\sigma,0) = 1 - C^0(\sigma,1), \quad C^1(\sigma,0) = -C^1(\sigma,1)$$

which are the global self-consistency conditions. By symmetry we find that the concentration tends to $\frac{1}{2}$ as σ tends to infinity, i.e.

$$C^0 \to \frac{1}{2} \quad \text{and} \quad C^1 \to 0 \quad \text{as} \quad \sigma \to \infty.$$

Notice the zeroth order solution to this problem is the same as the problem in the main body of this paper namely equations (35) and (36). However, the first order solution is given by

$$C^1 = \sqrt{\frac{2}{\pi}}\int_0^\infty \frac{e^{-k^2\tau}}{1+e^{-k^2}}\left(\int_0^\tau e^{k^2 z}\overline{E}\, dz - \int_\tau^1 e^{k^2(z-1)}\overline{E}\, dz\right)\sin(k\sigma)dk$$

where

$$\overline{E} = \mathcal{F}^s\left\{(1+P_\tau)\sigma C^0_{\sigma\sigma}\right\} = \sqrt{\frac{2}{\pi}}(1+P_\tau)\int_0^\infty \sigma C^0_{\sigma\sigma}\sin(k\sigma)\, d\sigma$$

$$= \left(\frac{2}{\pi}\right)^{\frac{3}{2}}(1+P_\tau)\int_0^\infty\int_0^\infty \frac{\sigma\lambda e^{-\lambda^2 z}}{e^{-\lambda^2}+1}\sin(\lambda\sigma)\sin(k\sigma)\, d\lambda d\sigma.$$

B Effective diffusivity

To obtain the effective diffusivity in the large Péclet number limit we can use the boundary layer coordinate to obtain

$$D_{\text{eff}} = -D\sqrt{\text{Pe}}\int_0^1 C_\sigma|_{\sigma=0}\, d\tau = D\sqrt{\text{Pe}}(I^0 + \text{Pe}^{-1/2}I^1 + O(\text{Pe}^{-1}))$$

where

$$I^0 = -\int_0^1 C^0_\sigma|_{\sigma=0}\, d\tau = \frac{2^{3/2}-1}{\pi^{3/2}}\zeta\left(\frac{3}{2}\right) \approx 0.85780470$$

$$I^1 = -\int_0^1 C^1_\sigma|_{\sigma=0}\, d\tau = \frac{4}{\pi^2}(1+P_\tau)\int_0^\infty\int_0^\infty\int_0^\infty \chi\lambda\sin(\lambda\chi)\Omega\sin(k\chi)\, d\lambda d\chi dk$$

where Ω is defined in equation (45). Applying our previous conjecture on I^1 to this expression gives us

$$I^1 = -\frac{1+P_\tau}{8}.$$

Substituting this into the effective diffusivity equation (42) yields

$$\frac{D_{\text{eff}}}{D\sqrt{\text{Pe}}} \approx 0.8578047 - \frac{1+P_\tau}{8}\text{Pe}^{-1/2} + O(\text{Pe}^{-1}). \tag{73}$$

References

Abramowitz, M., Stegun, I.A., 1968. Handbook of Mathematical Functions with Formulas, Graphs, and Mathematical Tables. US Government printing office.

Acrivos, A., Goddard, J.D., 1965. Asymptotic expansions for laminar forced-convection heat and mass transfer Part 1. Low speed flows. J. Fluid Mech. 23, 273–291.

Andereck, C.D., Liu, S., Swinney, H.L., 1986. Flow regimes in a circular Couette system with independently rotating cylinders. J. Fluid Mech. 164, 155–183.

Aris, R., 1956. On the dispersion of a solute in a fluid flowing through a tube. Proc. R. Soc. Lond. A 235, 66–77.

Bryden, M., Brenner, H., 1999. Mass-transfer enhancement via chaotic laminar flow within a droplet. J. Fluid Mech. 379, 319–331.

Butler, M., 2005. Animal cell cultures: recent achievements and perspectives in the production of biopharmaceuticals. Appl. Microbiol. Biotechnol. 68, 268–291.

Coles, D., 1965. Transition in circular Couette flow. J. Fluid Mech. 21, 385–425.

Esser, A., Grossmann, S., 1996. Analytic expression for Taylor–Couette stability boundary. Phys. Fluids 8, 1814–1819.

Ghosh, S., Chang, H.-C., Sen, M., 1992. Heat-transfer enhancement due to slender recirculation and chaotic transport between counter-rotating eccentric cylinders. J. Fluid Mech. 238, 119–154.

Godwin, L.E., Trevelyan, P.M.J., Akinaga, T., Generalis, S.C., 2023. Transient dynamics in counter-rotating stratified Taylor-Couette flow. Mathematics 11, 3250.

Grassia, P., Ubal, S., 2018. Streamline-averaged mass transfer in a circulating drop. Chem. Eng. Sci. 190, 190–219.
Helffrich, G.R., Wood, B.J., 2001. The Earth's mantle. Nature 412, 501–507.
Hristova, H., Roch, S., Schmid, P.J., Tuckerman, L.S., 2002. Transient growth in Taylor-Couette flow. Phys. Fluids 14, 3475–3484.
Nemri, M., Charton, S., Climent, E., 2016. Mixing and axial dispersion in Taylor-Couette flows: the effect of the flow regime. Chem. Eng. Sci. 139, 109–124.
Pithan, F., Svensson, G., Caballero, R., Chechin, D., Cronin, T., Ekman, A.M.L., Neggers, R., Shupe, M.D., Tjernström, A.S.M., Wendisch, M., 2018. Role of air-mass transformations in exchange between the Arctic and mid-latitudes. Nat. Geosci. 11, 805–812.
Pöschke, P., Sokolov, I.M., Zaks, M.A., Nepomnyashchy, A.A., 2017. Transport on intermediate time scales in flows with cat's eye patterns. Phys. Rev. E 96, 062,128.
Rosenbluth, M.N., Berk, H.L., Doxas, I., Horton, W., 1987. Effective diffusion in laminar convective flows. Phys. Fluids 30, 2636–2647.
Shraiman, B.I., 1987. Diffusive transport in a Rayleigh-Bénard convection cell. Phys. Rev. A 36, 261–267.
Siegel, C., 2008. Review of computational heat and mass transfer modeling in polymer-electrolyte-membrane (PEM) fuel cells. Energy 33, 1331–1352.
Taylor, G.I., 1923. Stability of a viscous liquid contained between two rotating cylinders. Philos. Trans. R. Soc. Lond. Ser. A 223, 289–343.
Taylor, G.I., 1953. Dispersion of soluble matter in solvent flowing slowly through a tube. Proc. R. Soc. Lond. A 219, 186–203.
Thiffeault, J.-L., 2012. Using multiscale norms to quantify mixing and transport. Nonlinearity 25, R1–R44.
Trevelyan, P.M.J., Kalliadasis, S., Merkin, J.H., Scott, S.K., 2002. Mass-transport enhancement in regions bounded by rigid walls. J. Eng. Math. 42, 45–64.
Wang, L., Sun, D-W., 2003. Recent developments in numerical modelling of heating and cooling processes in the food industry-a review. Trends Food Sci. Technol. 14, 408–423.
Zhang, Z., Wang, W., Qiu, B., 2014. Oceanic mass transport by mesoscale eddies. Science 345, 322–324.
Zhao, H., Yang, Y., Chen, Y., Li, J., Wang, L., Li, C., 2022. A review of multiple Pickering emulsions: solid stabilization, preparation, particle effect, and application. Chem. Eng. Sci. 248, 117085.